Modeling the role of the fluorine dopant in the magnetic phase diagram of LaFeAsO$_{1-x}$F$_x$ superconductors

Harry I. Fisher and Feliciano Giustino

Department of Materials, University of Oxford, Parks Road, Oxford OX1 3PH, United Kingdom

By using first-principles calculations we clarify the origin of the doping-induced transition from a stripe-antiferromagnetic phase to a nonmagnetic phase in LaFeAsO$_{1-x}$F$_x$. The explicit description of the F atoms in the calculations is found to be essential for reproducing the observed phase transition. Our study shows that the concerted effects of lattice distortion and band filling arising from the dopants act to lower the energy of an unoccupied band of predominant Fe d_{yz} character, until it crosses the Fermi level and the Fe magnetic moment is quenched.

I. INTRODUCTION

The discovery of superconductivity in LaFeAsO$_{1-x}$F$_x$ with a critical temperature T_c of 26 K generated considerable interest in the iron pnictides.[1] Substitution of La by other rare-earth elements has been found to lead to even higher T_c values, up to 55 K in F-doped SmFeAsO.[2] Other related iron-based compounds are also superconducting when doped, such as BaFe$_2$As$_2$,[3] LiFeAs,[4] and FeSe$_{1-\delta}$.[5] References 6 and 7 among others provide comprehensive reviews of the current state of the art in this area.

LaFeAsO crystallizes in the ZrCuSiAs-type structure (space group $P4/nmm$). As shown in Fig. 1, LaFeAsO consists of alternating layers of FeAs and LaO, and the tetragonal unit cell comprises two formula units. The a and c lattice parameters and the internal coordinates of the La and As atoms along the c axis are sufficient to fully describe the crystal structure. Resistivity,[8] neutron scattering,[9] and muon spin rotation measurements[10] in LaFeAsO indicate the onset of antiferromagnetism below the Néel temperature $T_N \sim 137$–150 K, and the nature of the magnetic order at low temperature is currently thought to be stripe antiferromagnetic.[11] Upon doping the antiferromagnetic parent compound LaFeAsO with F, the magnetic moment of Fe is quenched at a fluorine content corresponding to $x = 0.04$, and a superconducting state develops at $x = 0.05$.[10] This situation is reminiscent of the electronic phase diagram in copper oxide superconductors.[12] The proximity of a magnetic and a superconducting phase suggests that magnetism and superconductivity are closely related in LaFeAsO$_{1-x}$F$_x$ and other ferropnictides.[13]

Despite considerable efforts in the area of first-principles computational modeling of LaFeAsO$_{1-x}$F$_x$ and other iron-based superconductors, the atomistic mechanism underlying the magnetic phase diagram of these compounds remains an outstanding issue. For instance, while neutron scattering experiments yield a magnetic moment of $0.36\mu_B$ for the Fe atoms in LaFeAsO at $T = 8$ K,[9] the moment predicted by density-functional theory (DFT) calculations ranges between $0.8\mu_B$ and $2.6\mu_B$.[14–16] The origin of this discrepancy is still under debate.[17] The analysis of the magnetic phase diagram is further complicated by the strong sensitivity of the electronic ground state of LaFeAsO to the fine details of the crystal structure.[14] Most importantly, several attempts at modeling

the evolution of the magnetic ground state as a function of F doping in LaFeAsO$_{1-x}$F$_x$ (Refs. 18 and 19) consistently failed to reproduce the magnetic-nonmagnetic transition observed in experiment.[9,10]

In this work we show, using first-principles calculations, that the explicit inclusion of the F atoms in the modeling of LaFeAsO$_{1-x}$F$_x$ is crucial in order to obtain a magnetic-nonmagnetic phase transition as observed in the experiments. The role of the dopants is found to be twofold: (i) The F atoms induce structural distortions which act to reduce the As height and lower an unoccupied band of predominantly Fe d_{yz} character around the zone center towards the Fermi level. (ii) The extra electrons introduced by F populate this band and further lower its energy, leading to Fermi-level crossing and a suppression of the magnetic order.

The paper is organized as follows: In Sec. II we provide the details of our calculations. In Sec. III we demonstrate the necessity of including the F dopants using supercell calculations in order to correctly describe the magnetic-nonmagnetic transition in LaFeAsO$_{1-x}$F$_x$, and we develop a simplified model of the phase transition which captures the essential physics of the doping and is based on the unit cell of pristine LaFeAsO. In Sec. IV we discuss our findings in light of recent experimental and theoretical work, and in Sec. V we present our conclusions.

II. COMPUTATIONAL METHODS

We perform DFT calculations within the generalized gradient approximation of Ref. 20 using the Quantum ESPRESSO software package.[21] The valence electronic wave functions and charge density are described using plane-wave basis sets with kinetic energy cutoffs of 35 and 420 Ry, respectively. The core-valence interaction is taken into account by means of ultrasoft pseudopotentials[22] for La, As, O, and F. In the case of Fe we use the projector-augmented wave method.[23] We carry out structural optimizations until the force on each atom is below 10 meV/Å and the pressure is below 0.5 kbar. Most structural optimizations are performed using the standard Broyden-Fletcher-Goldfarb-Shanno method.[21] Occasionally during the relaxation, while the true ground state is magnetic, the system becomes trapped in a nonmagnetic local minimum. This effect arises from the connection between the As height
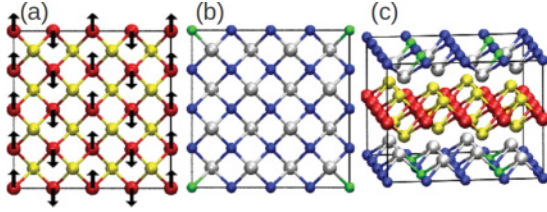
FIG. 1. (Color online) Ball-and-stick representation of LaFeAsO$_{1-x}$F$_x$. (a) Top view of the Fe-As layer in the $2\sqrt{2} \times 2\sqrt{2}$ unit cell, containing 16 FeAs units [Fe and As atoms in red (dark gray) and yellow (light gray), respectively]. The stripe-antiferromagnetic spin texture of the Fe atoms in pristine LaFeAsO is shown schematically. (b) Top view of the LaO layer [La and O atoms in silver (white) and blue (black), respectively], with one O atom replaced by F [green (gray)]. In this model corresponding to $x = 0.0625$ the nearest-neighbor distance between F dopants is 11.3 Å. (c) Lateral view of LaFeAsO$_{1-x}$F$_x$ with $x = 0.5$ and the F atoms in the most symmetric arrangement. The unit cell contains 64 atoms.

and the magnetic moment.[19] We here circumvent this difficulty by validating all our calculated structures and magnetic ground states using additional structural optimizations at fixed lattice parameters. We carry out an extensive set of calculations for LaFeAsO$_{1-x}$F$_x$ within the jellium model (JM), within the virtual-crystal approximation (VCA), and also by explicitly including the F atoms in the computational cell [explicit doping model (EDM)]. In the JM the negative charge of the doped electrons is compensated by a uniform positive background. For the VCA we generate ultrasoft pseudopotentials for the virtual atoms O$_{1-x}$F$_x$ using the ionic charge $Z_{O_{1-x}F_x} = 6 + x$.

For the calculations on the parent compound LaFeAsO and those on the doped compound within the JM and VCA, we adopt a $\sqrt{2} \times \sqrt{2}$ supercell in the FeAs plane. This is the smallest supercell which can support a stripe-antiferromagnetic ground state (see Fig. 1 for schematic representations of the structures used in this work). The Brillouin zone of this cell is sampled on a $6 \times 6 \times 5$ Monkhorst-Pack[24] grid. In the case of LaFeAsO our calculated ground-state atomic geometry, band structure, and Fermi surface are in agreement with previous studies.[14,15] The ground state is found to be stripe antiferromagnetic as expected,[11] and the calculated magnetic moment of $2.13\mu_B$ per Fe atom is within the range of previous first-principles calculations.[14–16]

III. RESULTS

Figure 2 shows that calculations within the JM or the VCA fail to reproduce the measured magnetic-nonmagnetic phase transition when increasing F doping. Even when considering a heavily doped compound such as LaFeAsO$_{0.5}$F$_{0.5}$, both the JM and the VCA yield a stripe-antiferromagnetic ground state as in LaFeAsO. Figure 2 also shows that within the JM and VCA the magnetic moment does not decrease as a function of the F content x, contrary to experimental observations.[10] We note that in two previous studies a magnetic phase transition was reported within the JM,[25] and within constrained DFT based on the VCA,[26] respectively. However, Ref. 25 relies on a localized double-zeta polarized (DZP) basis set, which is known to incorrectly describe the energetics of
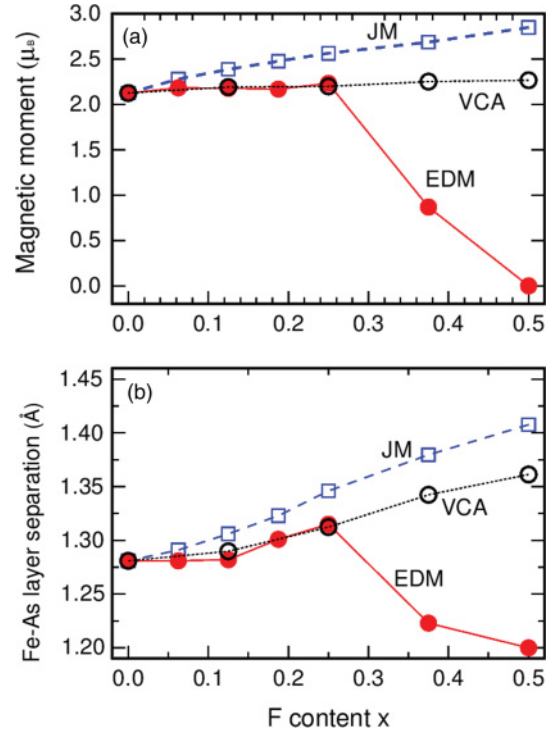

FIG. 2. (Color online) (a) Calculated magnetic moment per Fe atom in LaFeAsO$_{1-x}$F$_x$ as a function of F content x. The red disks correspond to the explicit doping model (EDM), the open blue squares correspond to the jellium model (JM), and the black circles are for the virtual-crystal approximation (VCA). The lines are guides to the eye. A magnetic-nonmagnetic phase transition is obtained only within the EDM. (b) Variation of the As height in LaFeAsO$_{1-x}$F$_x$ as a function of F content x. The red disks, blue squares, and black circles refer to the EDM, JM, and VCA calculations, respectively, and the lines are guides to the eye. The JM and VCA calculations yield incorrect structural trends. The EDM calculations reveal a compression of the Fe-As layer upon doping.

magnetic Fe.[27] Furthermore, unconstrained VCA calculations performed by some of the authors of Ref. 26 are in line with our results and demonstrate the failure of the VCA in LaFeAsO$_{1-x}$F$_x$.[18]

Prompted by the failure of the JM and VCA, we set out to determine whether EDM calculations, where the F atoms are explicitly included, can capture the mechanism underlying the phase transition observed in experiments. In order to include F atoms in our calculations we consider a larger supercell corresponding to $2\sqrt{2} \times 2\sqrt{2}$ unit cells (Fig. 1). This supercell contains 16 LaFeAsO formula units and allows us to investigate the effect of F corresponding to doping levels x which are multiples of $1/16 = 0.0625$. For consistency with the JM and VCA calculations the Brillouin zone of this large supercell is sampled on a $3 \times 3 \times 5$ Monkhorst-Pack grid. For a given doping level $x = n/16$ (n integer), n F atoms have to replace substitutionally an equal number of O atoms. It turns out that, even after taking into account the symmetry of the system, the number of possible inequivalent structures grows very rapidly with n. For example, we count 1, 5, and 16 inequivalent structures when replacing 1, 2, or 3 O atoms in the supercell by F, respectively.

Since the energy separation between magnetic and non-magnetic ground states is of only 12 meV/atom, all the calculations require *full* atomic and lattice optimizations and are computationally extremely intensive. As it would be practically impossible to analyze each and every dopant configuration, we here adopt an alternative strategy: (i) For each doping level, we sample a small subset of configurations, including the least and the most symmetric F patterns. (ii) We look for systematics within this small subset of configurations, and we formulate an hypothesis on the effect of the F dopants. (iii) We test this hypothesis by performing separate calculations which do not depend on the precise location of the F atoms. We consider a total of 14 F configurations. While this set of configurations is not statistically significant, it represents a useful starting point for pattern recognition.

Figure 2 shows that, within the EDM, the inclusion of the F dopant produces a phase transition with an onset at $x \sim 0.25$. At $x = 0.5$ the ground state of the system is nonmagnetic. We also observe that the $LaFeAsO_{1-x}F_x$ crystal structure is essentially unchanged up to $x = 0.25$. Above this dopant concentration the c axis shortens and the average As height is *reduced* from 1.31 Å ($x = 0$) to 1.20 Å ($x = 0.5$). In the nonmagnetic phase the F dopants induce a uniform contraction of the Fe and As planes. The compression of the c axis is consistent with powder x-ray diffraction data,[28] although the calculated contraction (0.33 Å) is more pronounced than in the experiment (0.04 Å). This is consistent with our overestimation of the magnetic moment of pristine LaOFeAs. We note that a previous theoretical study where the F dopants are explicitly included reports a nonmagnetic configuration at $x = 0.125$,[29] in apparent contradiction with the present results. However in Ref. 29 the calculations are spin unpolarized; hence they correspond to a local energy minimum, while we here address the magnetic ground state (which is spin polarized at $x = 0.125$, Fig. 2).

In order to identify the atomistic mechanism underlying the phase transition shown in Fig. 2, we investigate the correlation between magnetic moment and structural parameters. The only quantities which show a clear correlation are the As height (Fig. 3) and the c-axis length. A similar effect has been observed in neutron diffraction experiments on the related ferropnictide compound $CeFeAs_{1-x}P_xO$.[30] The correlation here determined between Fe magnetic moment and pnictogen height is in line with previous DFT calculations on LaFeAsO.[19]

We now want to develop the simplest possible model of $LaFeAsO_{1-x}F_x$ which is capable of reproducing the magnetic-nonmagnetic phase transition as obtained within the EDM in Fig. 2, but without incorporating the F atoms explicitly. Since the correlation in Fig. 3 suggests that the compression of the Fe-As layer is essential to the phase transition, we start from undoped LaFeAsO, and consider several modified structures with the same lattice parameters, but with the As height in the range of 1.20–1.35 Å as in the EDM calculations of Fig. 3. For each As height we consider two limiting cases: (i) the total number of electrons is as in pristine LaFeAsO, and (ii) the electron number is the same as in $LaFeAsO_{0.5}F_{0.5}$. The inset of Fig. 3 (blue filled squares) shows that when adding electrons to the compressed Fe-As layer within the JM the magnetic moment is quenched at a critical As height of 1.22 Å,
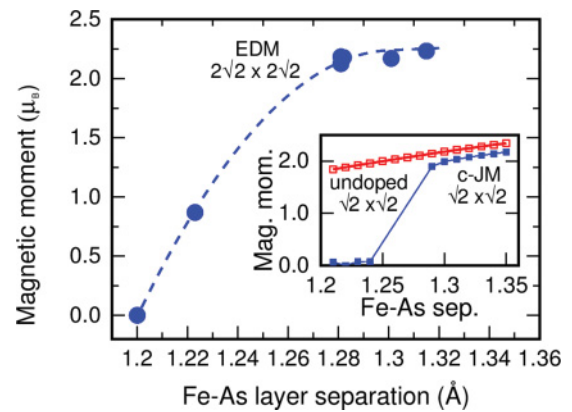

FIG. 3. (Color online) Calculated magnetic moment per Fe atom in $LaFeAsO_{1-x}F_x$ vs average Fe-As layer separation in the optimized ground-state geometry (blue disks), as obtained within the explicit doping model (EDM). The dashed line is a guide to the eye. Inset: Calculated magnetic moment per Fe atom vs Fe-As layer separation for the two cases of undoped LaFeAsO (open red squares) and of LaFeAsO with additional 0.5 electrons per Fe atoms (c-JM model for $x = 0.5$, blue filled squares). The lines are guides to the eye. The calculations in the main panel and in the inset correspond to the $2\sqrt{2} \times 2\sqrt{2}$ and the $\sqrt{2} \times \sqrt{2}$ unit cells, respectively.

in close agreement with our EDM calculations (Fig. 3). On the contrary, the electronic ground state of the modified LaFeAsO structure without the extra electrons is antiferromagnetic for all the As heights considered (open red squares in the inset of Fig. 3). These findings demonstrate that both the compression of the Fe-As layer and the presence of extra electrons crucially contribute to the suppression of the magnetic order. Since this result does not depend on the precise location of the F atoms in the supercell, this model provides an *a posteriori* justification to our EDM approach. We can summarize these findings by stating that the simplest model of the magnetic phase transition in F-doped LaFeAsO must include *both* the compression of the Fe-As layer and the presence of the F electrons within a jellium model. In the following we denote this JM with compressed Fe-As layer as "c-JM."

Now that we have a simple model of the doping-induced phase transition in LaFeAsO, we can analyze the underlying mechanism without the additional complication of the randomness introduced by dopants. Figure 4 shows the spatial distribution of the doped charge for the limiting case of $x = 0.5$ in three of the models considered here: EDM, JM, and c-JM. In both the EDM and c-JM models the doped charge exhibits substantial weight on the Fe d_{xy} and d_{yz} orbitals, while the $d_{x^2-y^2}$ orbitals are depleted (the x axis is aligned with the in-plane Fe-Fe direction). On the other hand, in the JM the extra electrons only occupy the Fe d_{yz} states. These observations are confirmed by detailed projected density of states analysis, and suggest that the band structures of the EDM and c-JM are in close agreement, while the JM model leads to an incorrect band filling. Similar calculations within the virtual-crystal approximation indicate that also the VCA leads to an incorrect band filling, similar to the JM.

Figure 5 shows the evolution of the band structure from pristine LaFeAsO to LaFeAsO with compressed FeAs layer,
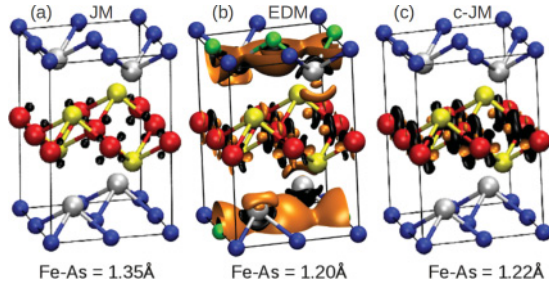
FIG. 4. (Color online) Charge density isosurfaces of doped electronic charge in LaFeAsO$_{1-x}$F$_x$ at $x = 0.5$. Excess (defect) electronic charge is represented in black [orange (gray)]. The color code for the ball-and-stick representations is the same as in Fig. 1. (a) Jellium model (JM) with the structure of pristine LaFeAsO (Fe-As layer separation 1.35 Å). The doped electrons incorrectly fill Fe d_{yz} states only. (b) Explicit doping model (EDM). In this case the optimized Fe-As layer separation is 1.20 Å. The doped electrons fill the Fe d_{xy} and d_{yz} states, and vacate the $d_{x^2-y^2}$ states. Additional charge rearrangement takes place in the F-doped LaO layer. (c) Simplified c-JM model where the Fe-As layer is compressed as in the EDM (separation: 1.22 Å), and extra electrons are added. The charge rearrangement in this case is very similar to the more sophisticated EDM calculation in (b).

and then to doped LaFeAsO within the c-JM model. Upon compression [Fig. 5(a) to Fig. 5(b)] an unoccupied band of predominantly Fe d_{yz} character shifts toward the Fermi level at Γ. When the dopant electrons are added [Fig. 5(b) to Fig. 5(c)] this band crosses the Fermi level.[31] Since from $x = 0$ to $x = 0.5$ the d_{yz} band near Γ shifts symmetrically across the Fermi level (Fig. 5), the magnetic phase transition that we identified at $x \sim 0.25$ in the EDM must be closely related to a Fermi-level crossing. We speculate that such Fermi-level crossing stabilizes the nonmagnetic phase by providing an additional screening channel to the second-nearest-neighbor Fe-Fe superexchange interaction.[15]
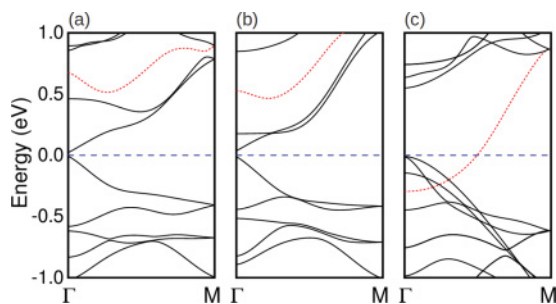

FIG. 5. (Color online) Band structures of LaFeAsO$_{1-x}$F$_x$ within the $\sqrt{2} \times \sqrt{2}$ unit cell. The Fermi level is indicated by the blue dashed line. The unoccupied band of predominantly Fe d_{yz} character discussed in the main text is highlighted in red (dotted line). (a) Pristine LaFeAsO. (b) Undoped LaFeAsO with compressed Fe-As layer. (c) c-JM model of LaFeAsO$_{1-x}$F$_x$ at $x = 0.5$. The band dispersing upward from Γ near the Fermi level in (a) and (b) has also d_{yz} character and merges into the red dotted curve in (c) upon suppression of the magnetic order. This is the only band which is filled upon doping in the JM model, as shown in Fig. 4(a).

IV. DISCUSSION

Due to the overestimation of the Fe magnetic moment in pristine LaFeAsO within DFT, the mechanism proposed here explains only qualitatively the magnetic phase transition in this compound. Indeed the phase transition identified here takes place for a F content which is about an order of magnitude larger than in experiment (calculated onset at $x = 0.25$ vs $x = 0.04$ in Ref. 10). This is consistent with the overestimation of the magnetic moment in LaFeAsO by approximately the same amount, and is in line with recent constrained-DFT calculations.[26] In order to reconcile calculations and experiment on pristine LaFeAsO, mechanisms based on spin fluctuations have been proposed in Refs. 17, 32, and 33. These proposals involve a suppression of the long-range magnetic order due to the increase of spin fluctuations with doping. We expect that, by combining our model with such proposals, a quantitative agreement with experiments will finally be achieved.

The mechanism proposed here may also explain the suppression of magnetic order in LaFeAsO upon application of pressure.[34] In LaFeAsO under pressure the c axis shortens and the As height is reduced,[35] similarly to the F-doped compound considered here. This similarity suggests a common origin for the suppression of magnetism upon F doping or upon application of pressure, respectively.

Our present findings carry implications for the study of electron-phonon interactions in superconducting LaFeAsO$_{1-x}$F$_x$. In fact according to our study the calculation of the electron-phonon coupling strength should be carried out within the c-JM with the compressed Fe-As layer, not within the structure of pristine LaFeAsO in the nonmagnetic LDA structure.[29,36] The same reasoning holds true for the development of low-energy Hamiltonians for LaFeAsO$_{1-x}$F$_x$,[37] which will need to take into account the modification of the electronic structure induced by the F dopants.

V. CONCLUSIONS

In conclusion, our work establishes the crucial role of the F atoms in driving the antiferromagnetic to nonmagnetic transition in LaFeAsO. In particular we have shown that, in order to reproduce the magnetic-nonmagnetic phase transition in LaFeAsO$_{1-x}$F$_x$ observed in the experiments, the standard virtual-crystal approximation is not sufficient and it is crucial to explicitly include F atoms in the calculations. In fact the F dopants not only introduce extra electrons, but also induce structural distortions which act to reduce the As height and modify the band structure of pristine LaFeAsO, leading to a Fermi-level crossing and a suppression of the magnetic order.

We also developed a simple jellium model for LaFeAsO$_{1-x}$F$_x$ which will enable more advanced calculations, based, for instance, on dynamical mean-field theory or GW techniques, using small unit cells and yet capturing the essential physics of the doping.

Incidentally, our work highlights the importance of carrying out very careful global optimizations involving all the lattice

degrees of freedom in order to identify the correct magnetic ground state in LaFeAsO$_{1-x}$F$_x$.

It is hoped that the present work will be useful for investigating the interplay between magnetism, lattice dynamics, and superconductivity in LaFeAsO. The generalization to other ferropnictides should not pose any difficulties.

[1]Y. Kamihara, T. Watanabe, M. Hirano, and H. Hosono, J. Am. Chem. Soc. **130**, 3296 (2008).

[2]R. Zhi-An, L. Wei, Y. Jie, Y. Wei, S. Xiao-Li, Zheng-Cai, C. Guang-Can, D. Xiao-Li, S. Li-Lung, Z. Fang, and Z. Zhong-Xian, Chin. Phys. Lett. **25**, 2215 (2008).

[3]M. Rotter, M. Tegel, D. Johrendt, I. Schellenberg, W. Hermes, and R. Pöttgen, Phys. Rev. B **78**, 020503 (2008).

[4]X. C. Wang, Q. Q. Liu, Y. X. Lv, W. B. Gao, L. X. Yang, R. C. Yu, F. Y. Li, and C. Q. Jin, Solid State Commun. **148**, 538 (2008).

[5]F.-C. Hsu, J.-Y. Luo, K.-W. Yeh, T.-K. Chen, T.-W. Huang, P. M. Wu, Y.-C. Lee, Y.-L. Huang, Y.-Y. Chu, D.-C. Yan, and M.-K. Wu, Proc. Natl. Acad. Sci. USA **105**, 14262 (2008).

[6]M. D. Lumsden and A. D. Christianson, J. Phys.: Condens. Matter **22**, 203203 (2010).

[7]J. Paglione and R. L. Greene, Nat. Phys. **6**, 645 (2010).

[8]J. Dong, H. J. Zhang, G. Xu, Z. Li, G. Li, W. Z. Hu, D. Wu, G. F. Chen, X. Dai, J. L. Luo, Z. Fang, and N. L. Wang, Europhys. Lett. **83**, 27006 (2008).

[9]C. de la Cruz, Q. Huang, J. W. Lynn, J. Li, W. Ratcliff II, J. L. Zarestky, H. A. Mook, G. F. Chen, J. L. Luo, N. L. Wang, and P. Dai, Nature (London) **453**, 899 (2008).

[10]H. Luetkens, H.-H. Klauss, M. Kraken, F. J. Litterst, T. Dellmann, R. Klingeler, C. Hess, R. Khasanov, A. Amato, C. Baines, M. Kosmala, O. J. Schumann, M. Braden, J. Hamann-Borrero, N. Leps, A. Kondrat, G. Behr, J. Werner, and B. Büchner, Nat. Mater. **8**, 305 (2009).

[11]S. Ishibashi, K. Terakura, and H. Hosono, J. Phys. Soc. Jpn. **77**, 053709 (2008).

[12]W. E. Pickett, Rev. Mod. Phys. **61**, 433 (1989).

[13]I. I. Mazin, D. J. Singh, M. D. Johannes, and M. H. Du, Phys. Rev. Lett. **101**, 057003 (2008).

[14]I. I. Mazin, M. D. Johannes, L. Boeri, K. Koepernik, and D. J. Singh, Phys. Rev. B **78**, 085104 (2008).

[15]Z. P. Yin, S. Lebègue, M. J. Han, B. P. Neal, S. Y. Savrasov, and W. E. Pickett, Phys. Rev. Lett. **101**, 047001 (2008).

[16]T. Yildirim, Phys. Rev. Lett. **101**, 057010 (2008).

[17]I. I. Mazin and M. D. Johannes, Nat. Phys. **5**, 141 (2009).

[18]G. Giovannetti, S. Kumar, and J. van den Brink, Physica B **403**, 3653 (2008).

[19]S. Lebegue, Z. P. Yin, and W. E. Pickett, New J. Phys. **11**, 025004 (2009).

[20]J. P. Perdew and Y. Wang, Phys. Rev. B **45**, 13244 (1992).

[21]P. Giannozzi, S. Baroni, N. Bonini, M. Calandra, R. Car, C. Cavazzoni, D. Ceresoli, G. L. Chiarotti, M. Cococcioni, I. Dabo, A. Dal Corso, S. de Gironcoli, S. Fabris, G. Fratesi, R. Gebauer, U. Gerstmann, C. Gougoussis, A. Kokalj, M. Lazzeri, L. Martin-Samos, N. Marzari, F. Mauri, R. Mazzarello, S. Paolini, A. Pasquarello, L. Paulatto, C. Sbraccia, S. Scandolo, G. Sclauzero, A. P. Seitsonen, A. Smogunov, P. Umari, and R. M. Wentzcovitch, J. Phys.: Condens. Matter **21**, 395502 (2009).

[22]D. Vanderbilt, Phys. Rev. B **41**, 7892 (1990).

[23]P. E. Blöchl, Phys. Rev. B **50**, 17953 (1994).

[24]H. J. Monkhorst and J. D. Pack, Phys. Rev. B **13**, 5188 (1976).

[25]F. Yndurain and J. M. Soler, Phys. Rev. B **79**, 134506 (2009).

[26]G. Giovannetti, C. Ortix, M. Marsman, M. Capone, J. van den Brink, and J. Lorenzana, Nat. Commun. **2**, 398 (2011).

[27]V. M. García-Suárez, C. M. Newman, C. J. Lambert, J. M. Pruneda, and J. Ferrer, J. Phys.: Condens. Matter **16**, 5453 (2004).

[28]A. S. Sefat, M. A. McGuire, B. C. Sales, R. Jin, J. Y. Howe, and D. Mandrus, Phys. Rev. B **77**, 174503 (2008).

[29]J. Noffsinger, F. Giustino, S. G. Louie, and M. L. Cohen, Phys. Rev. Lett. **102**, 147003 (2009).

[30]C. de la Cruz, W. Z. Hu, S. Li, Q. Huang, J. W. Lynn, M. A. Green, G. F. Chen, N. L. Wang, H. A. Mook, Q. Si, and P. Dai, Phys. Rev. Lett. **104**, 017204 (2010).

[31]In the c-JM for $x = 0.5$ we find that bands with d_{xy} and $d_{x^2-y^2}$ character have moved below and above the Fermi level, respectively. This is fully consistent with the charge redistribution observed in Figs. 4(b) and 4(c).

[32]S. Sharma, S. Shallcross, J. K. Dewhurst, A. Sanna, C. Bersier, S. Massidda, and E. K. U. Gross, Phys. Rev. B **80**, 184502 (2009).

[33]M. D. Johannes, I. I. Mazin, and D. S. Parker, Phys. Rev. B **82**, 024527 (2010).

[34]H. Okada, K. Igawa, H. Takahashi, Y. Kamihara, M. Hirano, H. Hosono, K. Matsubayashi, and Y. Uwatoko, J. Phys. Soc. Jpn. **77**, 113712 (2008).

[35]Y. Yang and X. Hu, J. Appl. Phys. **106**, 073910 (2009).

[36]L. Boeri, O. V. Dolgov, and A. A. Golubov, Phys. Rev. Lett. **101**, 026403 (2008).

[37]T. Miyake, K. Nakamura, R. Arita, and M. Imada, J. Phys. Soc. Jpn. **79**, 044705 (2010).

[38]W. Humphrey, A. Dalke, and K. Schulten, J. Mol. Graphics **14**, 33 (1996).